

A New Evaluation Method of Contact Area at Interface between Pulsed Surface Discharge and Water

Tomohiro Furusato, *Member, IEEE*, Daichi Obata, Yota Yamamoto, and Takahiko Yamashita, *Member, IEEE*

Abstract—The authors propose a new method for evaluating the contact area of a surface discharge on water by analyzing the resistance of water solution. This method supplements optical observations of light emissions and the Schlieren method. The contact area was modeled as a disk electrode, and the theoretical resistance of water was calculated under the assumption of a mutual similarity between the current and electrostatic fields. A simulated electrostatic field was calculated using a common charge-simulation method. Experimental values of the resistance of water were obtained by dividing the measured voltage drop at water by the measured current. The contact area evaluation was performed by comparing experimental and theoretical resistance values. The contact area increases with increasing applied voltage and is practically independent of water depth.

Index Terms—Surface discharge on water, pulsed power, discharge contact area, charge-simulation method, cathode fall voltage.

I. INTRODUCTION

SURFACE discharge on water with pulsed voltage is an effective method for wastewater treatment and production of polymers [1]-[3]. The propagation characteristics of a surface discharge are closely related to the chemical reaction that takes place in the water solution. Several researchers have investigated discharge propagation on the surface of water when a pulsed voltage is applied. M. Sato *et al.* [4] found that discharge propagation depends on the configuration of ground electrodes in water. N. Midi *et al.* [5] reported that the discharge length decreases with increasing conductivity of water. K. Yoshihara *et al.* [6] found that the surface discharge length is independent of the length of the air gap between the needle electrode and the water surface. However, the underlying mechanisms behind surface discharge are not yet understood completely.

Estimations of the contact area between a discharge and the water surface play a significant role in the examination of

The manuscript was submitted in March 2017 “This work was partially supported by JSPS KAKENHI Grant-in-Aid for Scientific Research (C) Grant Number JP16K06231”.

T. Furusato, Y. Yamamoto, S. Yamashita and T. Yamashita are with the Graduate School of Engineering, Nagasaki University, Nagasaki 852-8521, Japan (e-mail: t-furusato@nagasaki-u.ac.jp).

D. Obata is with the Department of Electrical Engineering, Nishinippon Institute of Technology, Fukuoka 880-0394, Japan (obata@nishitech.ac.jp).

discharge propagation and the chemical reactions that ensue. These estimations are also helpful for monitoring the discharge behavior on the solution surface in, for instance, a wastewater treatment system. The laser Schlieren technique or observation of plasma emissions have been typically used to measure discharge channels. The diameter of the discharge is inferred from the thermal diameter in the Schlieren method [7], [8] and the optical diameter when observing plasma emissions [9]. According to B. Jones, and R. T. Waters, the thermal and optical diameters of leader discharges differed significantly under the same gap length [10]. This difference poses an obstacle to accurate measurements of discharge areas.

This study proposes a novel method for measuring the discharge contact area on the basis of the analysis of voltage and current waveforms. This method correlates the discharge contact area with the resistance of the treated water. The resistance is calculated through Ohm’s law, taking the cathode fall voltage into account. The discharge contact area is modeled as a disk electrode with zero thickness. The relation between the resistance of water and the contact area is calculated under the assumption of a mutual similarity between the current and electrostatic fields. The electrostatic field is calculated through charge simulations. We found that the discharge contact area can be evaluated by comparison of the experimental and theoretical resistance.

II. EXPERIMENTAL SETUP AND PROCEDURE

A. Experimental Setup

Figure 1 shows a diagram of the experimental circuit with an illustration of how the discharge observation system was placed.

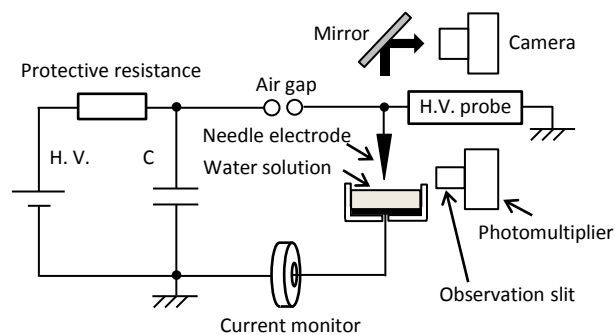


Fig. 1. Experimental circuit and discharge observation system.

The capacitor (2 nF) was charged by a DC power supply through a protective resistance. A positive pulsed voltage was applied to the needle-to-plane electrode by turning the self-breakdown gap switch on. A tungsten needle electrode was used to prevent erosion as much as possible. The setup included a high-voltage probe (Iwatsu Co. Ltd., HV-P30) and a current monitor (Pearson electronics Co. Ltd., model 4100) to measure voltage and current at the discharge. The conductivity of the water was adjusted by dissolving potassium chloride (KCl) and was set at 0.1 mS/cm for our tests. Discharges were observed via a mirror with a digital CMOS camera. Light emission from the discharge was observed with a photomultiplier tube (Hamamatsu Photonics K. K., 1P21) to obtain additional information about discharge propagation. Light emissions were observed through a slit. The spectral response of the photomultiplier tube is from 300 to 650 nm.

B. Equivalent Circuit Model of Experimental System

Figure 2 presents a simplified equivalent circuit diagram of the experimental setup and the air gap between the needle and water after the gap switch is turned on. The resistance of the discharge at the gap switch and the surface discharge are ignored in this model. The voltage drop of the surface discharge is mainly accounted for by the cathode fall voltage V_c for an electrolytic surface. The value of V_c has been reported to range from 1000 to 2000 V with a lightning impulse voltage applied [11]. Furthermore, the value of V_c originating from a pulsed surface discharge is higher than that from a DC glow discharge on water (400–800 V) [12]. The measurement method for the electrode fall voltage in this study is detailed in section III-B. A parallel circuit with variable resistance and capacitance can represent the water solution because the discharge contact area increases as the surface discharge propagates.

C. Evaluation Method of Discharge Contact Area

We propose a new method for measuring discharge contact area on the water that exploits the similarity between the current field in the water and an electrostatic field. The discharge contact area is modeled as a charged disk. A cross-section of this model is shown in Fig. 3. The charged disk is characterized by constant potential and zero thickness. The potential on the disk was calculated using a common charge-simulation method [13]. The current field was reproduced by arranging charged mirror disks at intervals of $2d$

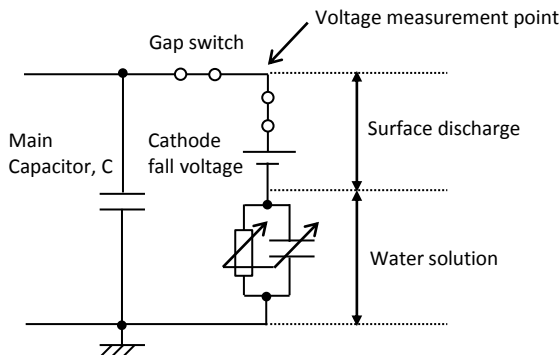


Fig. 2. A simplified equivalent circuit of experimental system after turning on a gap switch.

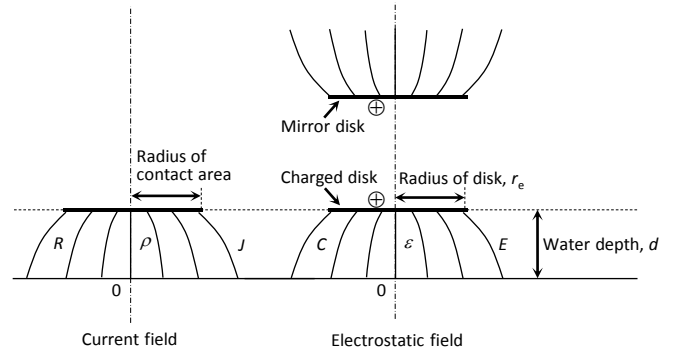


Fig. 3. A model of equivalent discharge contact area using disk and mirror electrodes with charge simulation method.

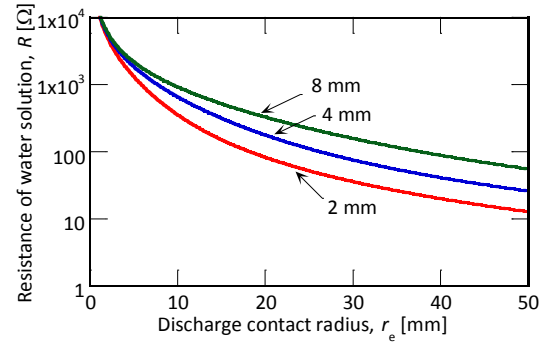


Fig. 4. Simulated resistance of water versus discharge contact radius.

(d : water depth) parallel to the charged disk. The capacitance C between the charged disk and ground under an arbitrary radius of the electrode is derived with calculations of the potential on the disk. Eventually, the resistance of water R can be derived by the following formula that assumes similarity between the current field and electrostatic one:

$$CR = \varepsilon\rho, \quad (1)$$

where ε is permittivity and ρ is resistivity of water. The dependence of the R on the radius of charged disk r_e is plotted in Fig. 4. The value of R decreases with increasing r_e for any value of d . The resistance of water was also measured experimentally. The details of the method used to measure the resistance using voltage and current waveforms are explained in section III-C. The calculated discharge contact area was evaluated by comparing the measured resistance and simulation results (Fig. 4).

III. RESULTS AND DISCUSSION

A. Discharge Propagation Characteristics

The maximum discharge length l_d is one of the important parameters that describe discharge propagation. Figure 5 plots l_d as a function of applied voltage. The value of l_d increases with increasing voltage peaks for each d . In the case of $d = 2$ mm and applied voltage of 20 kV, the value of l_d was slightly smaller than those with $d = 4$ or 8 mm. The propagation characteristics for each d were characterized by voltage and current waveforms as shown in Fig. 6 (a) and (b). Both voltage and

current pulse widths decrease with decreasing d . The narrow pulse at $d = 2$ mm is consistent with the short measured I_d .

B. Cathode Fall Voltage

Measurement of V_c is also important for calculating the discharge contact area. We focused on the discharge extinguishment of the gap switch, or the surface discharge, to measure V_c . Figure 7 shows a proposed model for the change of the equivalent experimental circuit at the moment of discharge extinguishment. The measured voltage is the sum of voltage drops at the surface discharge and the water solution. The dominant voltage drop of the surface discharge is V_c before discharge extinguishment, as discussed in section II-B. We assume that the charge of the main capacitor C is distributed to the capacitors at the gap switch and the needle-to-water surface during discharge extinguishment (see Fig. 7 [b]).

Figure 8 shows typical voltage and current waveforms including the period after discharge. A stepwise voltage

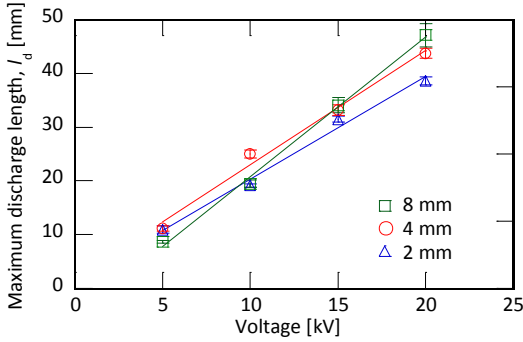
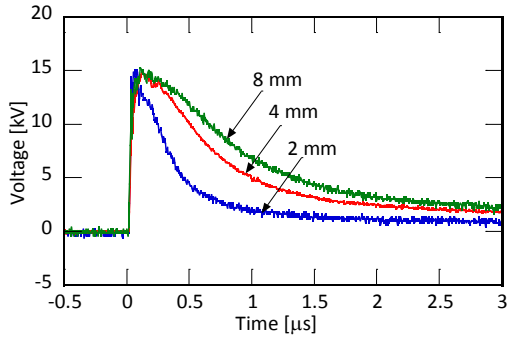
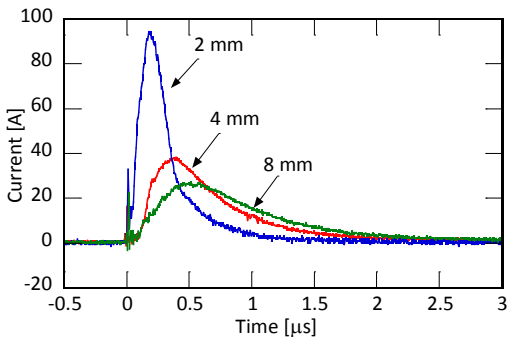


Fig. 5. Maximum discharge length as a function of the applied voltage for different water depth.

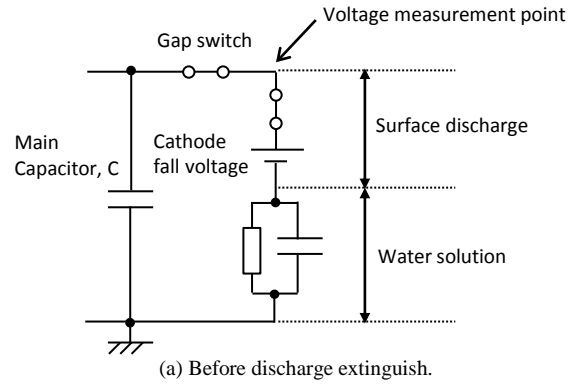


(a) Voltage waveforms.

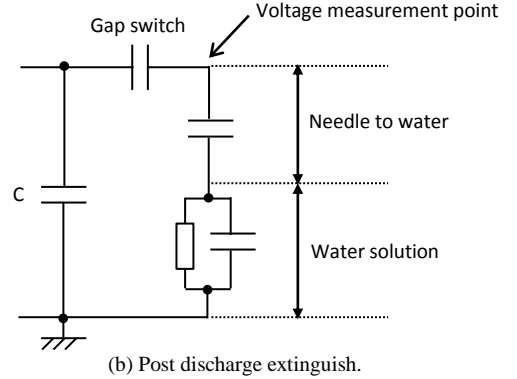


(b) Current waveforms.

Fig. 6. Voltage and current waveforms under same voltage peak.



(a) Before discharge extinguish.



(b) Post discharge extinguish.

Fig. 7. The change of a simplified equivalent experimental circuit due to the discharge extinguishing.

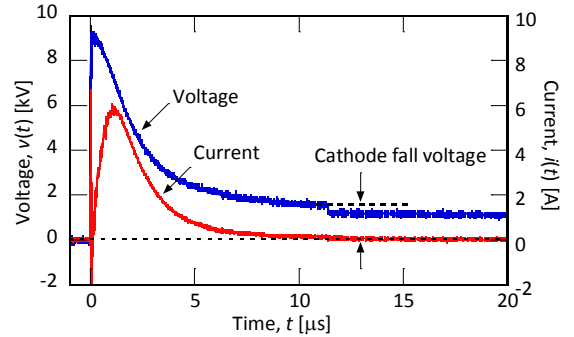


Fig. 8. Typical voltage and current waveforms including post discharge time under water depth of 8 mm.

variation suddenly appears during the voltage tail and indicates V_c . We suppose that the extinguishment of surface discharge occurs at the moment of the stepwise voltage variation. The stepwise voltage variation indicates the boundary between the situations in Figs. 7 (a) and (b). The voltage drop at the water solution should be taken into account when estimating V_c . The relaxation time τ of the water solution can be calculated as follows:

$$\tau = R(t)C(t) = \frac{\epsilon_0 \epsilon_r}{\sigma}, \quad (2)$$

where ϵ_0 is the permittivity of vacuum, ϵ_r is the relative permittivity of the water solution, and σ is the conductivity of the water solution. The calculated $\tau \sim 70$ ns was extremely small. Therefore, the capacitance of the water solution can be neglected at the time of the stepwise voltage variation. In

addition, the voltage drop due to the resistance of the water solution can also be ignored because the current hardly flows at the stepwise voltage variation. Consequently, the measured voltage immediately before the stepwise voltage variation can be approximated as equal to V_c . The measured V_c is nearly stable irrespective of the applied voltage at each d , as shown in Fig. 9. In the case of $d = 2$ mm, the value of V_c is slightly smaller than those for $d = 4$ and 8 mm.

C. Time Variation of Resistance of Water Solution and Light Emission of Discharge

The resistance of the water solution varies as the surface discharge propagates. The stop of the surface discharge propagation corresponding to l_d was estimated by resistance variation of water solution. The formula for variation in resistance $R(t)$, taking the cathode fall voltage into account, is as follows:

$$R(t) = \frac{v(t) - V_c}{i(t)}, \quad (3)$$

where $v(t)$ is the applied voltage, and $i(t)$ is the current. The displacement current in the water is neglected because of the short time of the process, $\tau \sim 70$ ns. The conduction current is dominant on this assumption. Figure 10 shows the time variations of light emission and the resistance of the water solution calculated using equation (3) with $d = 8$ mm. The direction of the observation slit of the photomultiplier was set toward the area around the tip of the discharge, approximately 20 mm from the needle electrode. The initial drastic decrease in $R(t)$ is due to the rapid propagation of the discharge. We

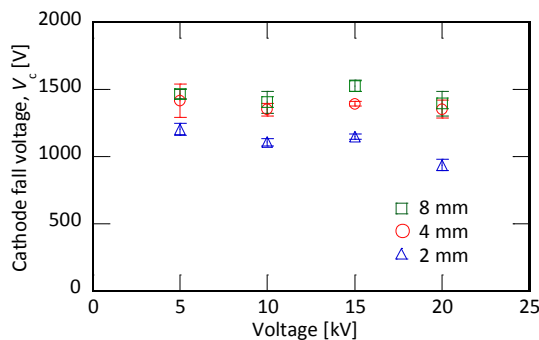


Fig. 9. The cathode fall voltage as a function of the applied voltage.

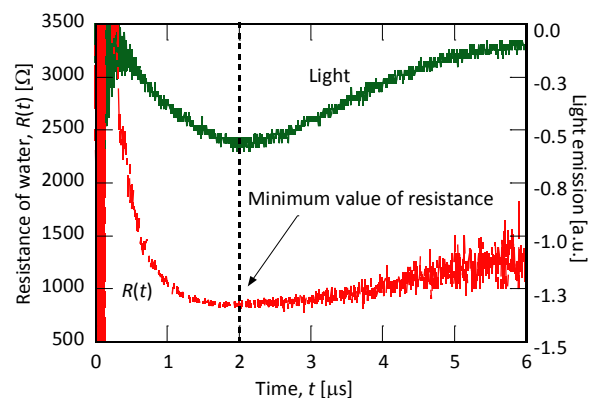


Fig. 10. Time variation of the resistance of water solution and light emission of the discharge (applied voltage: 10 kV, water depth: 8 mm).

suggest that the minimum value of $R(t)$ (R_{\min}) corresponds to the end of the surface discharge, because R_{\min} occurred at the same time as the peak of the light emission. The gradual increase of $R(t)$ after this moment suggests that the discharge shrinks before it ends. The value of R_{\min} is used to evaluate the discharge contact area in the charge-simulation method described in the next section.

D. Evaluation of Discharge Contact Area

The relation between the evaluated discharge contact area and the applied voltage is plotted in Fig. 11 for three different water depths. The contact area increases with increasing applied voltage for each d . Although the value of l_d at $d = 2$ mm is small compared with the conditions of $d = 4$ and 8 mm under relatively high applied voltages as shown in Fig. 5, the contact area is practically independent of d . We suggest that the streamer branching that depends on d affects the discharge contact area as well, following a previous study's suggestion that the magnitude of the conduction current in water is positively correlated with the field intensity along the water surface [14]. In addition, the intense electric field accelerates the electron detachment from the O_2^- and $O_2^-(H_2O)$ clusters around the tips of the discharge [15] and [16], and this leads to electron avalanches. We verified the effect of the current on the complexity of discharge branching with fractal analysis [14]. Figure 6 (b) shows current waveforms at different d under the same applied voltage peak. The current peak increases with decreasing d . We conclude that the streamer branching especially affects the discharge contact area with small d . Figure 12 shows processed binary images of experimentally measured surface discharges at each d under an applied voltage pulse of 5 kV. The image under the smallest $d = 2$ mm shows the highest degree of streamer branching, and this is consistent with the above explanation. However, these processed images were only used as a rough comparison with the evaluated

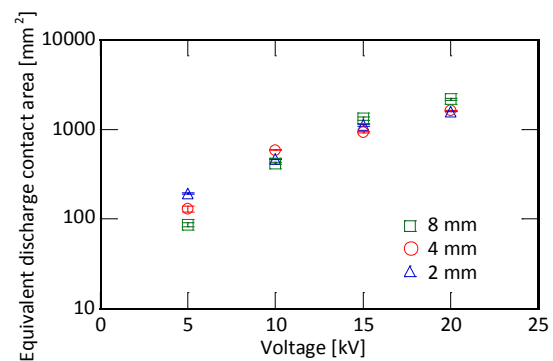


Fig. 11. Evaluated discharge contact area by means of charge simulation method as a function of applied voltage.

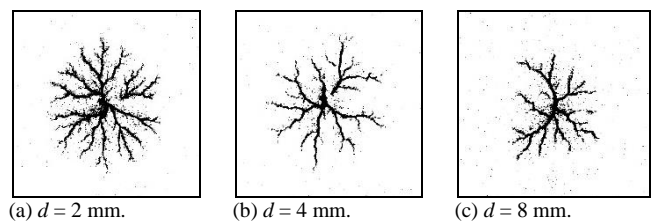


Fig. 12. Typical binary images of surface discharge depending on water depth under same applied voltage of 5 kV.

discharge contact area because the images are not sufficiently clear for accurate contact area measurements.

IV. CONCLUSION

The discharge contact area at the interface between a surface discharge and water solution was evaluated by means of a newly proposed evaluation method using voltage and current measurements and charge simulations. The area was evaluated quantitatively by comparing the measured and simulated resistance values for water. The results are summarized as follows.

- 1) The resistance of water was simulated using a model of a disk electrode. The value of resistance was calculated assuming mutual similarity between the current and electrostatic fields. The relation between the resistance of water and the radius of the modeled disk was simulated for various water depths.
- 2) The voltage drop at the water surface was calculated by subtracting the cathode fall voltage from the measured voltage. The resistance of water is this voltage drop divided by the discharge current. The variation of the resistance in time shows a concave curve. The stop time of a discharge was defined as the time of minimum resistance in the water, because this moment corresponds to the peak of light emission from the discharge. The minimum resistance was used to calculate the discharge contact area.
- 3) The evaluated discharge contact area increased with increasing applied voltage at each water depth. The contact area was hardly affected by the water depth except for the small voltage application.

ACKNOWLEDGMENTS

This work was partially supported by JSPS KAKENHI Grant-in-Aid for Scientific Research (C) Grant Number 16K06231.

REFERENCES

- [1] P. Lukes, and B. R. Locke, "Plasmachemical oxidation processes in a hybrid gas-liquid electrical discharge reactor," *J. Phys. D: Appl. Phys.*, vol. 38, no. 22, pp. 4074-4081, Nov. 2005.
- [2] S. Kanazawa, H. Kawano, S. Watanabe, T. Furuki, S. Akamine, R. Ichiki, T. Ohkubo, M. Kocik and J. Mizeraczyk, "Observation of OH radicals produced by pulsed discharges on the surface of a liquid," *Plasma Sources Sci. Technol.*, vol. 20, no. 3, 034010-1-034010-8, Jun. 2011.
- [3] Y. Hirano, R. Miyanomae, M. Sasaki, A. T. Quitain, T. Kida, and S. Okubayashi, "New Route for the Production of Thermosensitive Polymer with Pulsed Arc Discharge at the Argon-Water Interface," *IEEE Trans. Plasma Sci.*, vol. 44, no. 2, pp. 211-215, Feb. 2016.
- [4] M. Sato, T. Tokutake, T. Oshima, and T. Sugiarto, "Aqueous Phenol Decomposition by Pulsed Discharges on the Water Surface," *IEEE Trans. Ind. Appl.*, vol. 44, no. 5, pp. 1397-1402, Sep. 2008.
- [5] N. Midi, R. Ohyama, and S. Yamaguchi, "Underwater current distribution induced by spark discharge on a water surface," *J. Electrostat.*, vol. 71, no. 4, pp. 823-828, Aug. 2013.
- [6] K. Yoshihara, Ruma, S. H. R. Hosseini, T. Sakugawa, and H. Akiyama, "Study of Hydrogen Peroxide Generation by Water Surface Discharge," *IEEE Trans. Plasma Sci.*, vol. 42, no. 10, pp. 3226 - 3230, Oct. 2014.
- [7] R. Ono, and T. Oda, "Visualization of Streamer Channels and Shock Waves Generated by Positive Pulsed Corona Discharges using Laser Schlieren Method," *Jpn. J. Appl. Phys.*, vol. 43, no. 1, pp. 321-327, Jan. 2004.

- [8] T. Furusato, T. Ihara, T. Kiyam, S. Katsuki, M. Hara and H. Akiyama, "Initiation mechanism of a negative nanosecond pulsed discharge in supercritical carbon dioxide," *IEEE Trans. Plasma Sci.*, vol. 40, no. 11, pp. 3105-3115, Nov. 2012.
- [9] P. Bruggeman, E. Ribezl, A. Maslani, J. Degroote, A. Malesevic, R. Rego, J. Vierendeels, and C. Leys, "Characteristics of atmospheric pressure air discharges with a liquid cathode and a metal anode," *Plasma Sources Sci. Technol.*, vol. 17, no. 2, pp. 025012-1-025012-11, Apr. 2008.
- [10] B. Jones, and R. T. Waters, "Air insulation at large spacings," *Proc. Inst. Electr. Eng.*, vol. 125, no. 11, pp. 1152 - 1176, Nov. 1978.
- [11] T. Yamashita, H. Matsuo, H. Fujiyama, and T. Oshige, "Electrode-Fall of Local Discharge on an Electrolytic Surface," *IEEE Trans. Electr. Insul.*, vol. 23, no. 6, pp. 979-986, Dec. 1988.
- [12] P. Bruggeman, and C. Leys, "Non-thermal plasmas in and in contact with liquids," *J. Phys. D: Appl. Phys.*, vol. 42, no. 5, pp. 053001-1-053001-28, Feb. 2009.
- [13] M. Akazaki, K. Nishijima, and S. Sato, "Calculation of Three-Dimensional Axisymmetric Fields by Charge Simulation Method," *Electrical Engineering in Japan*, vol. 98, no. 4, pp. 1-7, Jul. 1978.
- [14] T. Furusato, T. Sadamatsu, Y. Matsuda, and T. Yamashita, "Streamer Branching and Spectroscopic Characteristics of Surface Discharge on Water under Different Pulsed Voltages," *IEEE Trans. Plasma Sci.*, Vol. 45, No. 4, pp. 711-717, Feb. 2017.
- [15] S. Badaloni and I. Gallimberti, "Basic data of air discharges," istituto di elettrotecnica e di elettronica, Univ. Padova, Padova, Italy, Tech. Rep. Upee-72/05, Jun. 1972.
- [16] N. Harid, and R. Waters, "Statistical study of impulse corona inception parameters on line conductors," *IEE Proc. A*, vol. 138, no. 3, pp. 161-168, May 1991.

Tomohiro Furusato (S'13-M'14) was born in Kagoshima, Japan, in 1988. He received the B. E., M. E., and Ph. D. degrees from Kumamoto University, Kumamoto Japan, in 2011, 2012, and 2014, respectively.



He was with the Japan Society for the Promotion of Science, Kumamoto University, from 2013 to 2014, as a Research Fellow. Since 2014, he has been an Assistant Professor with the Graduate School of Engineering, Nagasaki University, Nagasaki, Japan.



His research interests are pulsed-power, surface discharge, and discharge phenomena in supercritical fluids

Daichi Obata was born in Kagoshima, Japan, in 1988. He received the B. E., M. E., and Ph. D. degrees from Kumamoto University, Kumamoto Japan, in 2011, 2012, and 2015, respectively.

He worked for Kumamoto University as a Technical Assistant in 2015. Since 2016, he has been an Assistant Professor with the Department of Electrical Engineering, Nishinippon Institute of Technology, Fukuoka, Japan. His research interests are pulsed-power, electrostatics, and electrohydrodynamics.



Yota Yamamoto was born in Aichi, Japan, in 1995. He received the B.E. degree from Nagasaki University, Nagasaki, in 2016, where he is currently pursuing the M.E. degree.

His current research interests include surface discharge phenomena on water.



Takahiko Yamashita (M'00) was born in Fukuoka, Japan, in 1957. He received the B.E., M.E. and D.E. degrees from Kyushu University, Fukuoka, in 1980, 1982 and 1985, respectively.

He has been with Nagasaki University, Nagasaki, Japan, since 1985. He is currently a Professor of the Graduate School of Engineering and a Vice-President with Nagasaki University.

Dr. Yamashita is a Senior Member of the Institute of Electrical Engineers Japan